

Chapter 6

Convection and the Environment

In this final chapter we study the ways in which moist convection interacts with the surrounding atmospheric environment. Much of the material in this chapter is not as well understood as that in previous chapters, and is therefore more provisional and subject to future revision.

6.1 Quasi-equilibrium hypothesis

In our studies of turbulence, we found that turbulent eddies tended to have shorter time scales as one proceeds down in scale from that of the originating mechanism. This implies that once the originating mechanism is specified, the statistical characteristics of the turbulence are determined even though the details of turbulent flows are not.

One could view moist convection as a type of turbulence and therefore hypothesize that its statistical characteristics are similarly determined by convective forcing mechanisms. This approach has been used extensively in the statistical representation of convection in large-scale numerical models of the atmosphere where it is impractical to simulate the details of individual convective cells over a large, possibly global domain.

Emanuel et al. (1994; hereafter ENB) developed this idea in their paper on convective quasi-equilibrium (QE), though numerous QE-like models of convection precede their treatment. The underlying idea is that convection arises when there is convective instability, i.e., when the convective available potential energy (CAPE) is positive. Convection decreases CAPE by virtue of its tendency to rearrange atmospheric parcels in the vertical. QE occurs in

the view of Emanuel et al. (1994) when the tendency of convection to eliminate CAPE is balanced by the tendency of the surrounding environment to create it. As with ordinary turbulence, a necessary condition for QE to hold is that the time scale for convection to destroy CAPE must be significantly less than the time scale for the environment to create it.

A particularly simple form of the QE hypothesis introduced by ENB assumes that the convective time scale approaches zero, which means that convection destroys CAPE infinitely rapidly, resulting in an atmospheric state in which CAPE equals zero and the temperature profile is that characteristic of constant saturated moist entropy through the troposphere. The actual value of the saturated moist entropy is equal to the moist entropy of the boundary layer (the lowest few hundred meters of the atmosphere in which the potential temperature or dry entropy is nearly constant). The dynamics of the entire troposphere are therefore governed by the dynamics of the boundary layer in this case; once the temperature profile of the troposphere is determined, all other dynamical properties are determined. This model is called strict quasi-equilibrium or SQE.

A variation on SQE explored by ENB is that the convective relaxation time is short but finite (≈ 1 hr). This relaxation of SQE tends to damp large-scale, convectively coupled weather disturbances in the tropics.

An unanswered question relates to the factors controlling the moist entropy of the boundary layer. We will discuss this in more detail later. We simply note here that the existence of deep convection implies the production of precipitation-cooled downdrafts, which transport low-entropy air from aloft into the boundary layer, thus reducing the moist entropy there. This shifts the entire sounding, since the saturated moist entropy through the sounding is set equal to the boundary layer moist entropy. Since clear regions in the tropics are subject mainly to weak descent associated with radiative cooling, large-scale ascent is related primarily to ascent in convection. Thus, cooling of the boundary layer by downdrafts results in a correlation between large-scale ascent and a cooler troposphere. This is what would occur if ascent were dry entropy-conserving with dry entropy (or potential temperature) increasing upward. Thus, according to this model, strict quasi-equilibrium with downdrafts makes the convecting atmosphere behave as if it were dry, but with an effective Brunt-Väisälä frequency N_{eff} reduced from the dry value N :

$$N_{eff}^2 = (1 - \epsilon)N^2. \quad (6.1)$$

The quantity ϵ is characterized as a precipitation efficiency, i.e., one minus the fraction of precipitation reaching the surface without evaporating. If no precipitation evaporates, then $\epsilon = 1$ and the atmosphere is effectively neutral, with $N_{eff} = 0$. If it all evaporates, then $N_{eff} = N$ and the convection has basically no effect on large-scale dynamics. In between, N_{eff} is reduced somewhat from N .

The final factor in this picture is the effect of surface heat and moisture fluxes. Together, these fluxes create a flux of moist entropy into the boundary layer from the surface. This moist entropy flux can be represented approximately by a so-called bulk flux formula which takes the form

$$F_s = \rho_{bl} C_E U_{bl} (s_{ss}^* - s_{bl}) \quad (6.2)$$

over the ocean, where ρ_{bl} is the air density in the boundary layer, $C_E \approx 10^{-3}$ is the dimensionless exchange coefficient, U_{bl} is the boundary layer wind speed, s_{ss}^* is the saturated sea surface moist entropy at the temperature and pressure of the sea surface, and s_{bl} is the moist entropy in the boundary layer. The boundary layer entropy tends to become larger where the surface entropy fluxes are larger. Larger surface fluxes occur where the sea surface temperature is higher, increasing s_{ss}^* , and where the boundary layer wind speeds are stronger.

SQE is an elegant simplified theory that has greatly influenced thinking about the tropical atmosphere since the publication of ENB. However, it has also attracted significant criticisms, which we explore in the following sections.

6.2 Forcing of convection

Here we take a more mechanistic view of the formation of convection via the release of conditional instability. This release occurs when the convective inhibition (CIN) becomes small enough that random motions in the boundary layer are sufficient to lift a parcel through the layer of negative buoyancy to the level of free convection (LFC). If this happens, then the parcel then accelerates upward under its own positive buoyancy. The persistence of this upward acceleration depends on whether the parcel, which necessarily undergoes entrainment from the surrounding air, can maintain its buoyancy. Dry air in the environment is detrimental to the parcel's buoyancy.

The temperature difference between an ascending parcel and the surrounding environment is proportional to the difference between the saturated moist entropy values of the parcel and the environment. If the parcel is saturated, then the saturated moist entropy of the parcel equals the moist entropy, which in turn equals the mean moist entropy of the layer from which it originates for a non-entraining parcel, so that the saturated moist entropy difference of the saturated parcel relative to the environment is

$$\delta s^*(p) = s_p - s_e^*(p) \quad (6.3)$$

where s_p is the moist entropy of the parcel and $s_e^*(p)$ is the vertical profile of saturated moist entropy in the environment. The temperature difference in turn is

$$\delta T \approx \frac{\delta s^*}{\partial s_e^*(p)/\partial T}, \quad (6.4)$$

from which the virtual temperature difference can be calculated, given the mixing ratios of water vapor in the parcel and environment, r_p and r_e , and the mixing ratio of condensate in the parcel r_c (we assume that the environment is unsaturated):

$$\delta T_V = \delta T + [0.61(r_p - r_e) - r_c]T. \quad (6.5)$$

This equation employs an extended definition of virtual temperature which includes the effect of condensate on parcel density.

6.2.1 Forcing by lifting

The parcel-environment saturated moist entropy difference can be changed by changing either the boundary layer entropy or the environmental saturated moist entropy. The latter can be changed by dry adiabatic lifting of the environment via some large-scale process. Figure 6.1 shows how an initial sounding, shown by the red lines, changes when a small amount of lifting occurs, indicated by the thin purple arrows. The biggest change is in the saturated moist entropy, since the trajectories of the saturated entropy of environmental parcels follow lines of constant potential temperature, shown by the black contours. The result is an atmosphere with higher relative humidity that is more unstable to moist convection, and a reduction in the level of free convection, as indicated by downward displacement of the intersection of the green line representing the moist entropy of surface air with the saturated moist entropy curve. This shows that convective inhibition and

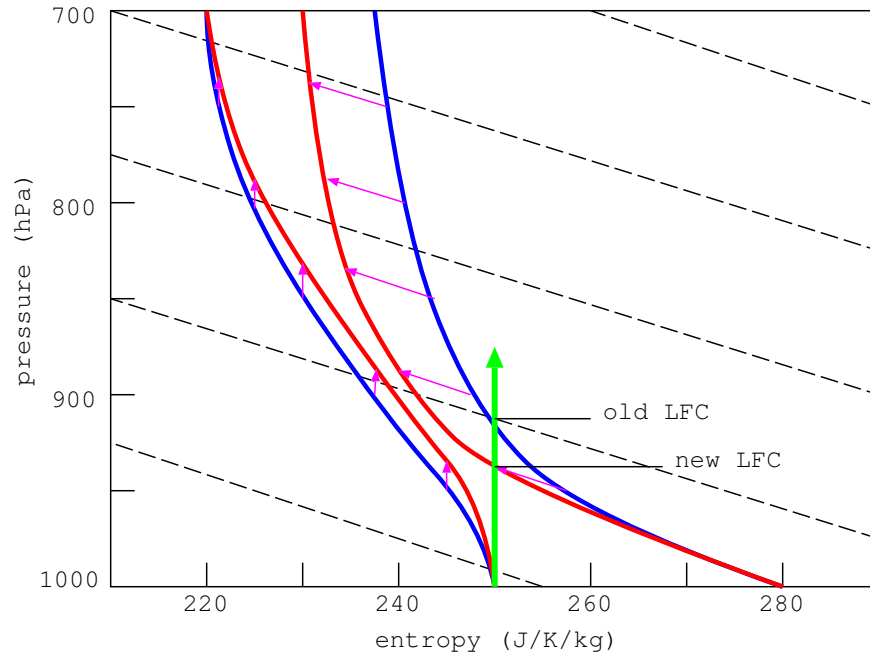


Figure 6.1: Effect on a sounding of dry adiabatic lifting. If the atmosphere is lifted by the amount shown by the purple arrows, the initial sounding shown in blue is transformed into the red sounding. The moist entropy remains constant in the lifting while the saturated moist entropy curve moves slantwise upwards along constant potential temperature lines, shown by the black dashed contours. The LFC of a surface parcel after the lifting is lower than the initial LFC. The CIN decreases drastically as a result of the lifting and the CAPE increases.

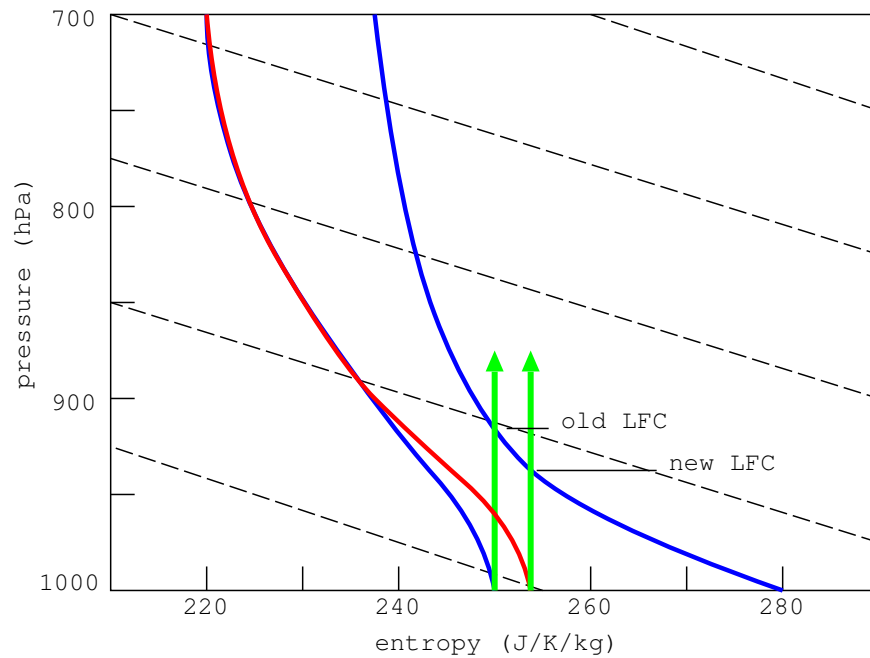


Figure 6.2: Effect on a sounding due to increased boundary layer specific moist entropy resulting from surface heat and moisture fluxes. The original sounding is shown in blue, the modified sounding in red. Lifting of a parcel from the surface results in the LFC being reached at a lower elevation for the modified sounding, with a smaller value of CIN.

convective available potential energy are very sensitive to small vertical displacements of the atmospheric column. These displacements can be caused by quasi-geostrophic motions in middle latitudes or gravity wave motions in the tropics.

6.2.2 Flux destabilization

Figure 6.2 shows the effect on the sounding of increasing the boundary layer moist entropy, as indicated by the blue line. The LFC for a parcel lifted from the surface decreases with higher boundary layer moist entropy, as illustrated in this figure. The CIN also decreases, as indicated by the decrease in the area below the LFC between the environmental and parcel profiles of saturated moist entropy.

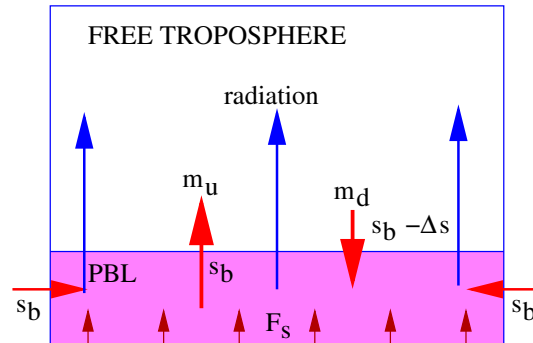


Figure 6.3: Flows of entropy in and out of the boundary layer (modified from Raymond et al. 2009).

6.3 Alternative forms of quasi-equilibrium

Recently Raymond and Herman (2011) challenged the validity of tropospheric QE on the basis of physical and modeling arguments. The essence of these arguments is that the only process that can act sufficiently rapidly to restore the environmental profile of temperature to a moist adiabat or some other equilibrium shape is the condensation and evaporation of water vapor; conservative advective processes were thought to be too slow. Numerical modeling of convection subjected to transient temperature anomalies in the upper and lower troposphere showed that the return to equilibrium in the upper troposphere is much slower than in the lower troposphere where there is much greater potential for condensation and evaporation to occur. Thus, rapid convective adjustment of environmental profiles of temperature appears to be possible in the lower troposphere but not the upper troposphere according to these results.

6.3.1 Boundary layer quasi-equilibrium (BLQ)

Raymond (1995) and Emanuel (1995) proposed that the atmospheric boundary layer exists in a state of quasi-equilibrium (irrespective of what happens in the free troposphere), with a balance between surface moist entropy fluxes, which tend to increase the boundary layer moist entropy, and radiation, entrainment, and convective downdrafts, which tend to decrease it. In Raymond's picture, the primary balance is between deep convective downdrafts

and surface fluxes:

$$F_s = M_d \delta s_d \quad (6.6)$$

where F_s is the flux of entropy into the boundary from below, M_d is the mass per unit area per unit time of downdraft air entering the boundary layer and δs_d is the difference between the specific moist entropy in boundary layer and downdraft air.

A further assumption is that the downdraft mass flux M_d is equal on the average to some fraction α of the updraft mass flux out of the boundary layer, M_u :

$$M_d = \alpha M_u. \quad (6.7)$$

Both δs and α are assumed to be functions of the convection, which in turn depends on the convective environment. Combining equations (6.6) and (6.7) results in an expression for the convective updraft mass flux out of the boundary layer:

$$M_u = \frac{F_s}{\alpha \delta s_d}. \quad (6.8)$$

Thus, convection increases with increased surface entropy fluxes, driven by higher sea surface temperatures and stronger winds, smaller downdraft to updraft ratios, and a smaller difference between boundary layer and downdraft moist entropy.

The above analysis shows the important role played by downdrafts in controlling the amount of convection, and hence precipitation. If the downdraft-updraft ratio α goes to zero, then equation (6.8) tells us that the updraft mass flux goes to infinity! This, of course would not occur; some other mechanism of convective control would take over.

6.3.2 Lower tropospheric quasi-equilibrium (LTQE)

Based on a rather clever use of cloud-resolving models, Kuang (2008a,b) concluded that a form of convective quasi-equilibrium existed in which convection was thought to return only the lower troposphere rapidly to a saturated moist entropy profile locked to the boundary layer moist entropy. (Kuang actually used moist static energy in place of moist entropy, but the concept is the same.) This is a more general forcing mechanism than BLQ, because lower tropospheric forced lifting can generate convection in addition to surface entropy fluxes.

An equivalent extension of boundary layer quasi-equilibrium would be to extend the analysis to the non-equilibrium case by setting the updraft mass flux proportional to the difference between the boundary layer moist entropy s_{bl} and the saturated moist entropy of the throttling layer of the free troposphere s_{th}^* . This is the layer in which CIN acts and is generally found just above the boundary layer:

$$M_u = \gamma(s_{bl} - s_{th}^*). \quad (6.9)$$

The constant of proportionality γ controls how sensitive the updraft mass flux is to variations in boundary layer entropy and the free tropospheric saturated moist entropy in the throttling layer. Taking the time derivative of this equation, we obtain

$$\frac{dM_u}{dt} = \gamma \left[\frac{ds_{bl}}{dt} - \frac{ds_{th}^*}{dt} \right] = \gamma \left[\frac{F_s - \alpha M_u \delta s_d}{\rho_{bl} b} - \frac{ds_{th}^*}{dt} \right] \quad (6.10)$$

where b is the boundary layer thickness, ρ_{bl} is the air density in the boundary layer, and where F_s etc. are defined in the section on boundary layer quasi-equilibrium. Using $s^* = C_{PD} \ln \theta + Lr^*/T_F$, the time derivative of s_{th}^* (at constant pressure) can be written

$$\frac{ds_{th}^*}{dt} = \frac{ds_{th}^*}{d\theta} \frac{d\theta}{dt} = \frac{C_{PD}}{\theta} \left[1 + \frac{L^2 r^*}{R_V T C_{PD} T_F} \right] \frac{d\theta}{dt} \quad (6.11)$$

where we have used $d \ln e_s / dT = L / (R_V T^2)$. If the potential temperature θ is decreasing due solely to dry adiabatic lifting, then

$$\frac{d\theta}{dt} = -w_{th} \frac{d\theta}{dz} \quad (6.12)$$

where w_{th} is the vertical velocity in the throttle layer, which shows that

$$\frac{ds_{th}^*}{dt} = -\chi w_{th} \quad (6.13)$$

where

$$\chi = C_{PD} \frac{d \ln \theta}{dz} \left[1 + \frac{L^2 r^*}{C_{PD} R_V T T_F} \right]. \quad (6.14)$$

Assuming that all time derivatives are slow compared to the first term on the right side of this equation recovers BLQ. An extension of BLQ is to

assume that dM_u/dt is small compared to the other terms, but that ds_{th}^*/dt is not, implying that the right side of equation (6.10) is zero. Solving for the vertical mass flux in this case yields

$$M_u = \frac{F_s + \rho_{bl} b \chi w_{th}}{\alpha(\delta s_d)}. \quad (6.15)$$

This extended version of BLQ thus takes into account the possible destabilization of convection by dry adiabatic lifting, which as shown previously can release conditional instability.

6.4 Form of convection

Once convection is triggered by events in the boundary layer or just above, the question arises as to what controls the form of the resulting convection. The free tropospheric profiles of temperature, humidity, and wind are the only factors likely to come into play. Below we consider first the effects of temperature and humidity profiles and then those of wind shear.

6.4.1 Thermodynamic effects

It seems plausible that the higher the humidity, the more likely it is to rain. Observations support this argument. Bretherton et al. (2004) used satellite microwave sounding data to infer the mean precipitation rate as a function of column relative humidity or saturation fraction (S ; called r by Bretherton et al.), defined as follows:

$$S = \int_0^h \rho r_V dz / \int_0^h \rho r^* dz \quad (6.16)$$

where h is the height of the tropopause, $\rho(z)$ is the vertical profile of air density, $r_V(z)$ is the water vapor mixing ratio, and $r^*(z)$ is the saturation mixing ratio. The saturation fraction also can be characterized as the precipitable water (the thickness of the liquid water layer if all vapor condensed out to the surface) divided by the saturated precipitable water. Figure 6.4 shows Bretherton et al. (2004)'s results, which indicate that the precipitation rate is a steeply increasing function of saturation fraction. Other methods of measuring rainfall rate and saturation fraction show similar results, e.g.,

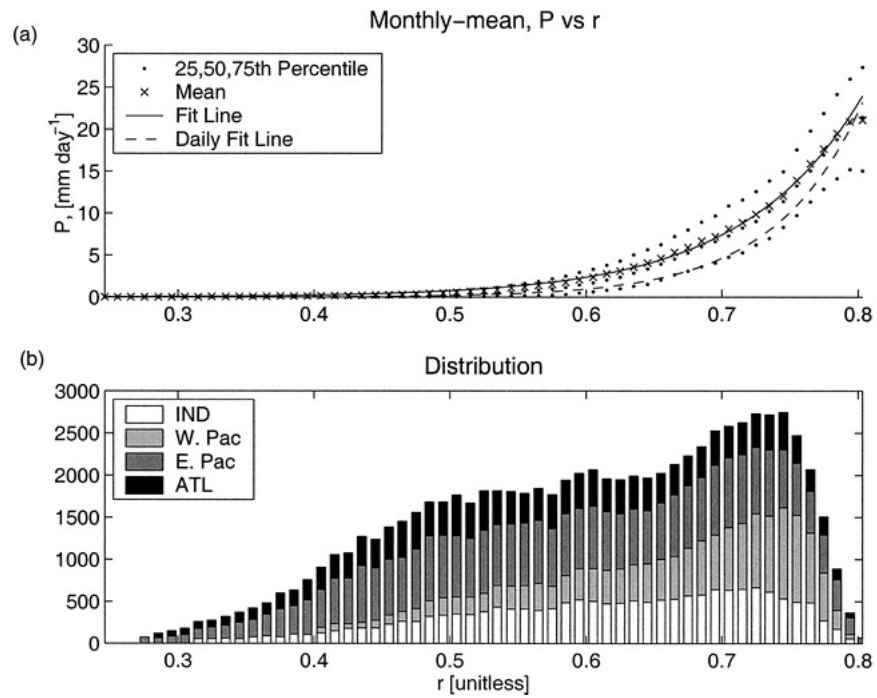


Figure 6.4: From Bretherton et al. (2004); satellite-derived precipitation rate as a function of column relative humidity or saturation fraction (upper panel); relative frequency of saturation fraction in different tropical ocean basins (lower panel).

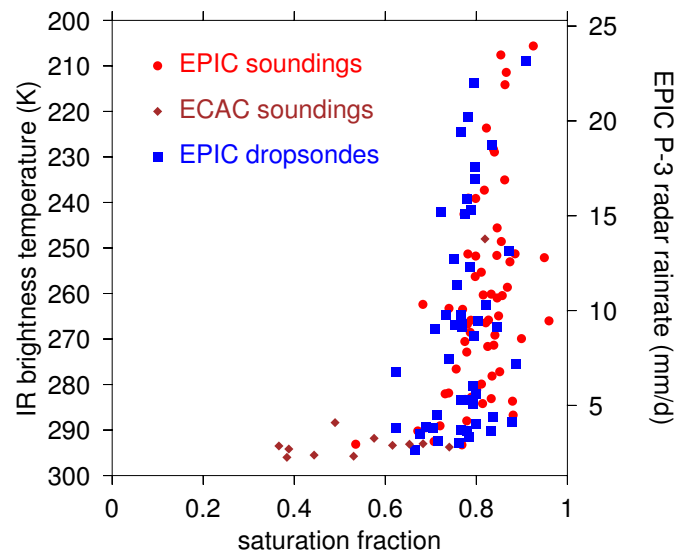


Figure 6.5: Satellite infrared brightness temperature as a proxy for rainfall rate as a function of saturation fraction derived from soundings of different sources in the eastern tropical Pacific and the southwest Caribbean (Raymond et al. 2007).

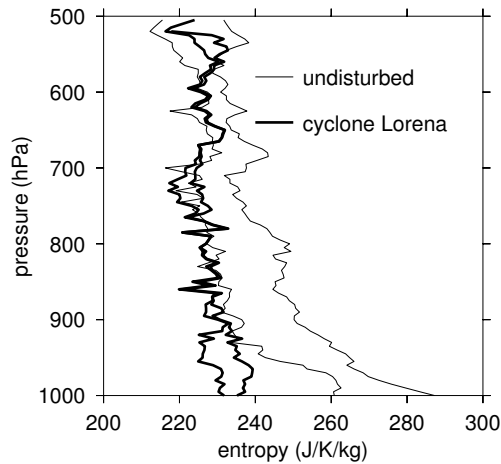


Figure 6.6: Comparison of observed soundings in the tropical east Pacific for undisturbed tropical conditions (thin lines) and for the environment of a developing tropical cyclone (thick lines).

from aircraft and ship soundings taken in conjunction with satellite infrared brightness temperature measurements, which can be related to rainfall rates measured by meteorological radar (Raymond et al. 2007; see figure 6.5).

The temperature profile as well as the humidity profile can also influence the form of convection. Bister and Emanuel (1997) postulated that a moister, more stable environment reduces convective downdrafts, thus suppressing the divergence in the horizontal wind at low levels that normally arises from these downdrafts. This suppression is thought to be important in promoting the spinup of tropical cyclones. Figure 6.6 shows how the sounding in an undisturbed tropical environment differs from that in the environment of a developing tropical cyclone (east Pacific tropical cyclone Lorena 2001). The cyclone environment has almost neutral moist convective instability and near-100% relative humidity.

In the oceanic tropics, the export of energy to middle latitudes is only a small part of the energy budget of the atmosphere. This budget consists primarily of a balance between the energy inflow from the ocean (which in turn is fed by the absorption of solar radiation) and the outflow of infrared radiation from upper levels of the atmosphere. The convection is responsible for transporting this energy from near the surface to the upper troposphere. There is also near-balance between evaporation and precipitation in the oceanic

tropics. Since most of the energy entering the atmosphere is in the form of latent heat, i.e., evaporation of water from the ocean surface, there is also a link between the precipitation rate and the energy entering the atmosphere from the surface. Local equilibrium in these budgets of energy and water substance, i.e., a steady-state situation with negligible lateral transport in or out of the domain of interest, is called radiative-convective equilibrium (RCE). The profiles of temperature and moisture that develop under these circumstances are called RCE profiles. These profiles can be computed in a cloud-resolving model (CRM) with closed or periodic lateral boundary conditions by letting the model run to equilibrium with suitable formulations for surface fluxes and outgoing thermal radiation imposed.

Raymond and Sessions (2007) used a CRM with so-called weak temperature gradient (WTG) lateral boundary conditions to simulate the effects of various perturbations to undisturbed oceanic tropical conditions on the resulting convection. These conditions were approximated by RCE simulations as discussed above. The resulting profiles resulting from these simulations are designated “reference profiles”.

WTG boundary conditions relax the mean vertical profile of potential temperature in the CRM domain to reference profiles that are selected to represent the convective environment. The cooling needed to effect this relaxation in the face of convective latent heat release is interpreted as that resulting from the adiabatic cooling associated with large-scale ascent called the “weak temperature gradient vertical velocity”, denoted w_{WTG} . The WTG vertical mass flux is the density times this vertical velocity, $M_{WTG}(z) = \rho w_{WTG}$. Mass continuity with this vertical mass flux profile is imagined to draw in air to the CRM domain laterally from the environment at appropriate levels with properties of the reference profile. Air is then expelled laterally at needed levels, depending on the requirements of mass continuity. These vertical and horizontal flows together represent a “parameterized” large-scale flow.

Figure 6.7 shows the patterns of WTG vertical mass flux associated with the perturbations to the RCE reference profiles shown in figure 6.8. The righthand panels in the two figures show, as expected, that when the reference profile is moistened relative to RCE, the vertical mass flux increases, which implies additional precipitation. The elevation of maximum vertical mass flux does not change significantly, remaining near 8 km. However, when the potential temperature profile is altered to have a warm anomaly in the upper troposphere and a cool anomaly in the lower troposphere, the strength

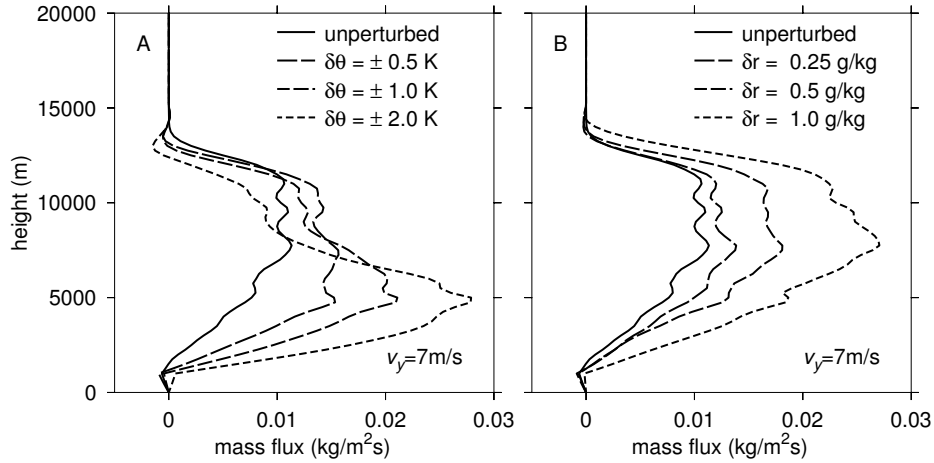


Figure 6.7: Computed WTG vertical mass flux profiles arising from the potential temperature $\delta\theta$ and mixing ratio δr perturbations shown in figure 6.8 (Raymond and Sessions 2007).

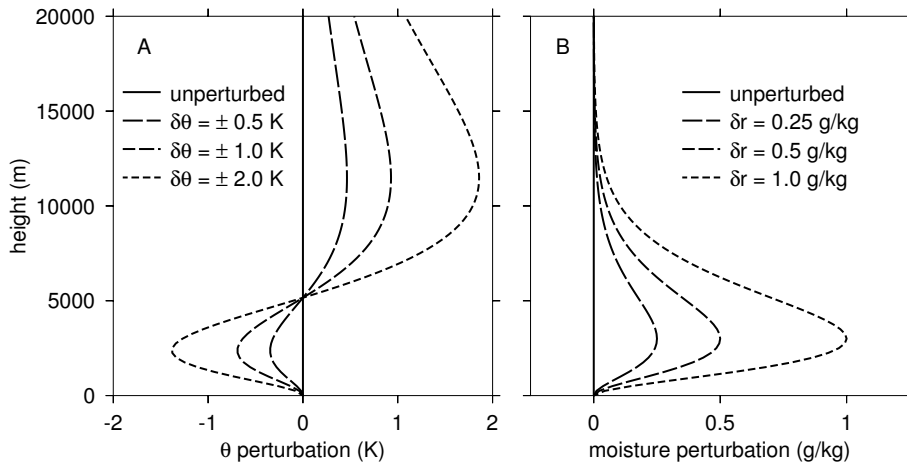


Figure 6.8: Perturbation profiles used in the calculations of Raymond and Sessions (2007).

of the vertical mass flux not only increases, but the elevation of maximum vertical mass flux also decreases to near 5 km in the most extreme case. Decreasing the mid-level convective instability by increasing the vertical gradient of potential temperature at mid-levels thus has the effect of creating shallower convection with stronger low-level inflow. Such a change appears to have important implications for the formation of tropical cyclones (Raymond et al. 2011).

6.4.2 Wind shear effects

The form of the environmental wind profile in which a convective cell or system of convective cells is embedded can affect the form and dynamics of convection. Figure 6.9 illustrates three common types of storm systems.

Multi-cell systems generally exist in weak shear and consist of a quasi-random array of convective cells in various stages of evolution. The mechanism by which convective cells generate further convective cells is the gust front, or the outflow of cold air at the surface resulting from precipitation-cooled downdrafts. This cold air spreads out, lifting unstable air in its path to the level of free convection, thus initiating new convective cells. This is perhaps the most common type of convective system.

Squall lines are linear arrays of convective cells organized by the dynamics of strong, low-level wind shear. The orientation of the line of cells may be perpendicular to the wind shear or at some angle, but never parallel to the shear. The system moves rapidly down-shear, initiating new convective cells on the down-shear side of the line. Cells generally move less rapidly than the line, thus passing back through the line as they evolve, dissipating at the rear of the line. The cool downdraft air is well-organized by the shear, producing the strong lifting on the down-shear side needed to generate new cells there. A sub-class of the multi-cell storm also exists in strong shear, in which the cells are aligned with the shear vector. Such storms are generally weaker than squall lines and typically do not move rapidly.

Supercell storms are very large single cells which exhibit cyclonic rotation. They occur in environments with strong winds and shear that changes direction with height, as shown in figure 6.9. The dynamics of such systems depends less on cold air outflows from downdrafts and more on the dynamics of rotation. Supercell storms are associated with the formation of large hail and strong tornados.

This section represents only the barest outline of the effects of wind shear

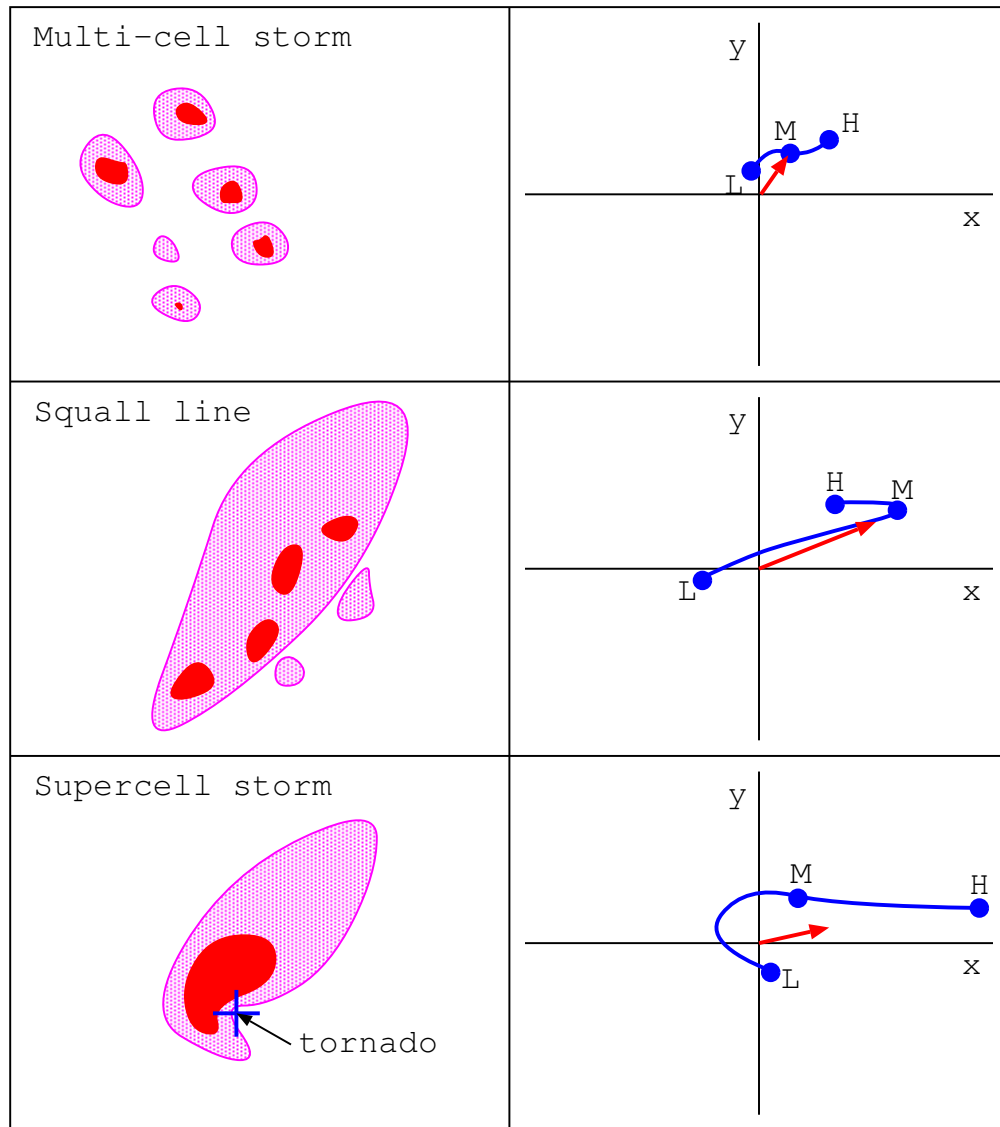


Figure 6.9: Types of storms associated with different wind hodographs, represented by the blue lines on the right. Each point on a hodograph line represents the tip of a wind vector relative to the origin. The labeled blue circles represent winds at low, middle, and high levels. The red arrows represent storm propagation velocities. The typical appearance of each type of storm system is shown in the left panels.

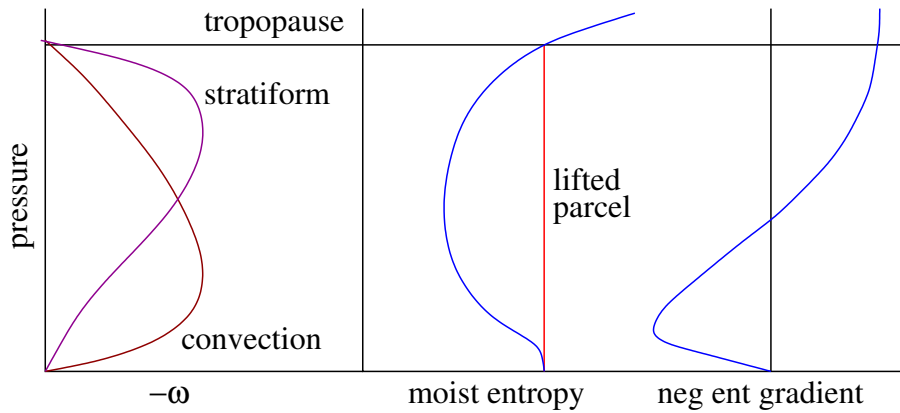


Figure 6.10: Factors entering into the numerator of the NGMS (from Raymond et al. 2009; see text for further explanation).

on deep moist convection. A good source for further study is the text by Houze (1994).

6.5 Convective aggregation and gross moist stability

So far in this chapter we have addressed the effects of the environment on the convection. In this last section we inquire about the reverse question; what effect does the convection have on the environment? In particular, how does the action of the convection affect the prospects for subsequent convection?

A useful concept in addressing this question is the gross moist stability (GMS), first introduced by Neelin and Held (1987). Roughly speaking, the GMS is the ratio between the lateral export of moist entropy (or moist static energy in Neelin and Held's treatment) and some measure of convective strength such as rainfall rate or vertical mass flux. Originally just a clever diagnostic, the GMS associated with convection becomes more valuable if it can be predicted based on the character of the convective environment. In the steady state, the lateral export of moist static energy equals the net vertical import of this quantity due to the surface moist entropy fluxes and the loss of entropy due to radiative processes. Given this moist entropy source and the GMS, the strength of the convection can be predicted.

Neelin and Held's (1987) version of GMS is based on a two-layer model

of the atmosphere and furthermore is not a non-dimensional quantity. A non-dimensional version of the GMS denoted the normalized GMS (NGMS) was defined by Raymond et al. (2009) in a manner that makes it useful in a real as opposed to idealized atmosphere. It is given by

$$\Gamma = -\frac{T_R [\nabla \cdot (s\mathbf{v})]}{L [\nabla \cdot (r\mathbf{v})]} \quad (6.17)$$

where Γ is the NGMS, T_R is a constant reference temperature characteristic of the atmosphere, L is the latent heat of evaporation, ∇ is the horizontal divergence, \mathbf{v} is the horizontal wind, s is the specific moist entropy, and r is the water vapor mixing ratio. The square brackets indicate a vertical integral in pressure from the surface to the tropopause.

The vertically integrated horizontal divergence of water vapor in the denominator of equation (6.17) is closely related to minus the precipitation rate. As such, it is negative in convective regions. The numerator of this equation is a bit trickier to understand. We first write

$$[\nabla \cdot (s\mathbf{v})] = [\mathbf{v} \cdot \nabla s] + [s\nabla \cdot \mathbf{v}]. \quad (6.18)$$

Using the mass continuity equation in pressure coordinates

$$\nabla \cdot \mathbf{v} + \frac{\partial \omega}{\partial p} = 0, \quad (6.19)$$

where $\omega = dp/dt$ is the pressure vertical velocity, we note that

$$[s\nabla \cdot \mathbf{v}] = -\left[s \frac{\partial \omega}{\partial p}\right] = -\left[\frac{\partial s\omega}{\partial p}\right] + \left[\omega \frac{\partial s}{\partial p}\right]. \quad (6.20)$$

The first term on the right side of equation (6.20) is zero if ω is zero at the surface and tropopause as a result of the integration in pressure. Equation (6.18) can therefore be rewritten under this assumption as

$$[\nabla \cdot (s\mathbf{v})] = [\mathbf{v} \cdot \nabla s] + \left[(-\omega) \left(-\frac{\partial s}{\partial p}\right)\right]. \quad (6.21)$$

The first term represents mainly external advective effects that occur when the horizontal mean wind relative to the convection is non-zero. As such, it is a manifestation of a large-scale effect largely independent of the

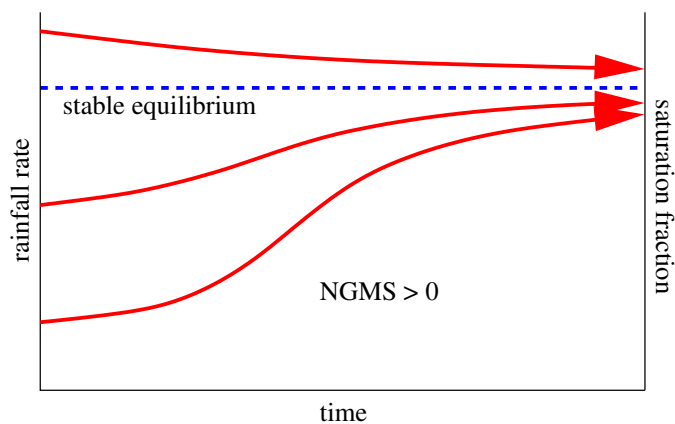


Figure 6.11: Response of convection to a perturbation in rainfall rate for uniformly positive NGMS (Raymond et al. 2009).

action of the convection. The second term, on the other hand, is controlled by the mass flux profile in the convective region, written here in pressure coordinate form as $\omega(p)$. Figure 6.10 reveals (upon close scrutiny – note that pressure decreases upward!) that the integrand in the second term has cancelling components in the lower and upper troposphere, with positive values in the upper troposphere and negative values in the lower troposphere. For top-heavy mass flux profiles, as in the stratiform case, the positive part of the integrand dominates, whereas for bottom-heavy convective mass flux profiles negative part dominates or comes close to dominating the positive part. Thus, top-heavy case makes the second term in equation 6.10 large, whereas it is smaller or negative for a bottom-heavy mass flux profile. Therefore, for large NGMS the net lateral export of moist entropy is large and the yield of precipitation for given surface flux and radiation values is small. In contrast, small NGMS means that much larger precipitation rates occur for given surface flux and radiation.

The above analysis is only valid in the time-independent, equilibrium case. Away from equilibrium, one needs to take into account the full, vertically integrated entropy equation:

$$\frac{\partial [s]}{\partial t} + [\nabla \cdot (s\mathbf{v})] = F_s - R, \quad (6.22)$$

where F_s is the surface entropy flux and R is the vertically integrated radiative sink of entropy. (The irreversible generation of entropy is ignored here,

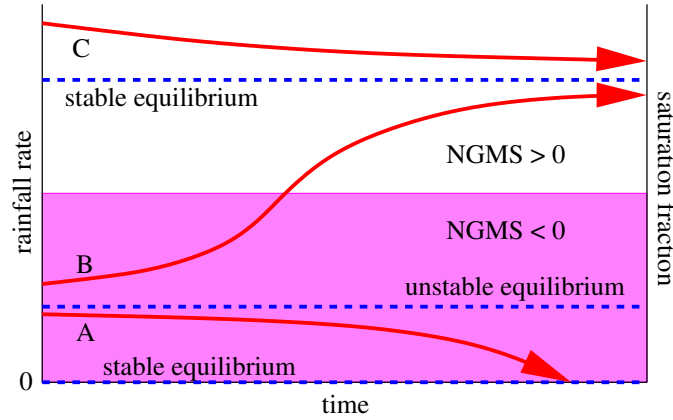


Figure 6.12: Response of convection to a perturbation in rainfall rate for the case of NGMS in dry conditions (Raymond et al. 2009).

but it could be included.) Assuming for now that the horizontal advection term is not important, we may write

$$[\nabla \cdot (s\mathbf{v})] = \frac{LP}{T_R}\Gamma \quad (6.23)$$

where we have approximated minus the integrated horizontal divergence of water vapor by the precipitation rate P . Rewriting equation (6.22), we get

$$\frac{\partial [s]}{\partial t} = -\frac{LP}{T_R}\Gamma + F_s - R. \quad (6.24)$$

If precipitation rate is a monotonically increasing function of saturation fraction, it also increases with increasing moist entropy if the temperature profile does not change much. Equilibrium occurs when the right side of this equation equals zero. However, if the precipitation somehow becomes slightly larger than its equilibrium value, then the time tendency of vertically integrated moist entropy is non-zero. If the NGMS is positive, this increase in precipitation tends to reduce the moist entropy, thus returning the precipitation toward its equilibrium value. If on the other hand $\Gamma < 0$, then the opposite occurs: a positive feedback loop tends to drive the precipitation to larger and larger values. The opposite occurs if the initial precipitation fluctuation is negative, driving the precipitation (and the saturation fraction) toward ever smaller values.

Figure 6.11 illustrates what happens if the NGMS is uniformly positive; deviations in the rainfall rate of any magnitude are eliminated as the system tends toward a stable equilibrium rainfall rate.

In real world, tropical oceanic environments, the NGMS tends to become negative for dry environments (López and Raymond 2005) and is positive for moister conditions. In this case multiple equilibria exist, with one equilibrium state being very dry with zero precipitation. Figure 6.12 illustrates this situation. Sessions et al. (2010) investigated this case in detail using a cloud-resolving model with weak temperature gradient boundary conditions. The existence of multiple equilibria may result in the self-aggregation of convection with large dry areas in between convective clusters.

6.6 References

- Bretherton**, C. S., M. E. Peters, and L. E. Back, 2004: Relationships between water vapor path and precipitation over the tropical oceans. *J. Climate*, **17**, 1517-1528.
- Houze**, R., 1994: *Cloud dynamics*, Elsevier Science, 573 pp.
- Kuang**, Z., 2008a: Modeling the interaction between cumulus convection and linear gravity waves using a limited-domain cloud system-resolving model. *J. Atmos. Sci.*, **65**, 576-591.
- Kuang**, Z., 2008b: A moisture-stratiform instability for convectively coupled waves. *J. Atmos. Sci.*, **65**, 834-854.
- López Carrillo**, C., and D. J. Raymond, 2005: Moisture tendency equations in a tropical atmosphere. *J. Atmos. Sci.*, **62**, 1601-1613.
- Raymond**, D. J., and M. J. Herman, 2011: Convective quasi-equilibrium reconsidered. *J. Adv. Model. Earth Syst.*, **3**, Art. 2011MS000079, 14 pp.
- Raymond**, D. J., S. L. Sessions, and Ž. Fuchs, 2007: A theory for the spinup of tropical depressions. *Quart. J. Roy. Meteor. Soc.*, **133**, 1743-1754.

Raymond, D. J., S. L. Sessions, and C. López Carrillo, 2011: Thermodynamics of tropical cyclogenesis in the northwest Pacific. *J. Geophys. Res.*, **116**, D18101, doi:10.1029/2011JD015624.

Raymond, D. J. and S. L. Sessions, 2007: Evolution of convection during tropical cyclogenesis. *Geophys. Res. Letters*, **34**, L06811, doi:10.1029/2006GL028607.

Raymond, D. J., S. Sessions, A. Sobel, and Ž. Fuchs, 2009: The mechanics of gross moist stability. *J. Adv. Model. Earth Syst.*, **1**, art. #9, 20 pp.

Sessions, S. L., S. Sugaya, D. J. Raymond, and A. H. Sobel, 2010: Multiple equilibria in a cloud-resolving model using the weak temperature gradient approximation. *J. Geophys. Res.*, **115**, D12110, doi:10.1029/2009JD013376.

6.7 Problems

UNDER CONSTRUCTION.